Defiducialization: Providing Experimental Measurements for Accurate Fixed-Order Predictions

A. Glazov

Deutsches Elektronen-Synchrotron DESY, Hamburg

Defiducialization: Providing Experimental Measurements for Accurate Fixed-Order Predictions

A. Glazov[*]

Deutsches Elektronen-Synchrotron DESY, Hamburg, Germany

Abstract

An experimental procedure is proposed to perform measurements of differential cross sections which can be compared to fixed-order QCD predictions with improved accuracy. The procedure can be applied to the Drell-Yan cross-section measurements which are differential in the boson transverse momentum. An example analysis is performed using the ATLAS measurement of the Z-boson production cross section at center-of-mass energy of 8 TeV. The resulting full phase space measurement of the cross section differential in the boson rapidity is compared to theoretical predictions computed with next-to-next-to leading-order accuracy in QCD.

I. INTRODUCTION

Accurate knowledge of parton distribution functions of the proton (PDFs) is essential for the physics program at the LHC. PDF uncertainties are the leading source of systematics for precision measurements of the W-boson mass and effective weak mixing angle, $\sin^2 \theta_W$ [1, 2]. Reduction of the PDF uncertainties is important in particular for the interpretation of high statistics measurements for the future LHC data.

PDFs can be constrained using W- and Z-boson production in the charged and neutral current Drell-Yan processes. These processes can be measured with sub-percent experimental accuracy and thus provide a valuable input for the PDF determination. An example of an accurate measument is the ATLAS result on γ^*/Z- and W-boson production at the center-of-mass energy of $\sqrt{s} = 7$ TeV [3]. For the Z boson, the measurement is perfromed in bins of the invariant mass of the lepton pair, $m_{\ell\ell}$, and of the lepton pair rapidity, $y_{\ell\ell}$. For the W boson, the results are reported as a function of the lepton pseudorapidity, η_ℓ. Excluding the global normalisation uncertainty, the measurement reaches better than 0.5% experimental uncertainty.

The cross sections differential in $y_{\ell\ell}$, $m_{\ell\ell}$ and η_ℓ are known at next-to-next-to leading-order (NNLO) accuracy in perturbative QCD [4–8]. For these observables, the corresponding computations are inclusive in the boson transverse momentum p_T and thus insenstive to $\ln p_T/m_{\ell\ell}$ divergences, providing a robust input for determination of collinear PDFs. However the ATLAS measurement is performed in a fiducial volume with experimental cuts on the lepton transverse momentum and lepton pseudorapidity which are required due to the detector acceptance. These selection criteria introduce dependence on p_T modelling thereby spoiling accuracy of the fixed-order predictions. The study performed in Ref. [3] shows that predictions become unstable with respect to small variations of the cuts and differ as much as 1% for different subtraction methods which is significant compared to the experimental accuracy.

The impact of the fiducial cuts on fixed-order predictions is under investigation since some time. It is known to be large when transverse momentum of individual leptons (or jets) approaches half of the invariant mass of the lepton pair (or jet pair). It has been proposed in Ref. [9] to introduce an asymmetry for the cut values for the leading and sub-leading objects. This procedure stabilizes the computation of the fixed-order predictions, however it does

not elliminate the uncertainty arising from the logarithmic corrections [10]. Computation of higher order corrections and/or inclusion of the $\ln p_T/m_{\ell\ell}$ resummation should reduce the uncertainty arising from the fiducial cuts. However the full next-to-next-to-next-to leading-order (N^{3}LO) corrections for Drell-Yan processes are not availible yet, while resummation corrections may bring additional uncertainties from the recoil prescirption [11].

Experimentally, it is sometimes possible to isolate regions in the phase space which are not affected by fiducial cuts. For example, in Ref. [12] the fiducial acceptance for the triple differential measurement of $\frac{d\sigma}{dy_{\ell\ell}d\cos\theta dm_{\ell\ell}}$, where $\cos\theta$ is the lepton polar angular variable, is above 99% for $|\cos\theta| < 0.4$, $y < 1$ and $m_{\ell\ell} > 66$ GeV [13]. This region can be safely compared to fixed-order predictions. Other experimental methods include explicit correction to the full phase space during the data analysis, as in e.g. Ref. [14].

In this paper, another approach is proposed. It is based on an observation that an acceptance correction from the fiducial to full phase space can be determined accurately using fixed-order calculations for the vector boson plus jet process for measurements given in bins of p_T. It is demonstrated in the following using the ATLAS measurement of Z-boson production differential in $y_{\ell\ell}$ and p_T performed using data collected at $\sqrt{s} = 8$ TeV [15]. The acceptance correction is computed at NLO for the Z plus jet process ($O(\alpha_S^2)$, where α_S is the strong coupling constant), using the MCFM v6.8 program [16], interfaced to APPLGRID [17]. The correction is used to determine the full phase space measurement differential in $y_{\ell\ell}$ and p_T. The result is integrated in p_T and the inclusive $d\sigma/dy_{\ell\ell}$ differential cross-section measurement is compared to the NNLO ($O(\alpha_S^2)$) computation for inclusive Z-boson production obtained using the MCFM v9 program [18, 19]. The paper concludes with a discussion of the results and possible applications of the method to other measurements.

II. FORMALISM

The fully differential Z-boson production cross section can be expressed as

$$\frac{d^5\sigma}{dp_T dy_{\ell\ell}dm_{\ell\ell}d\cos\theta d\phi} = \frac{3}{16\pi}\frac{d^3\sigma^{U+L}}{dp_T dy_{\ell\ell}dm_{\ell\ell}}\sum_{i=0}^{8}P_i(\cos\theta, \phi). \tag{1}$$

Here ϕ is the lepton azimuthal angular variable, $P_i(\cos\theta, \phi)$ are the nine harmonic polynomials, and σ^{U+L} is the unpolarised cross section. The harmonic polynomials depend on eight angular coefficients $A_i(p_T, y_{\ell\ell}, m_{\ell\ell})$ which define fractions of helicity cross sections with

respect to the unpolarised case. Equation 1 relies on factorization of the Z boson production and decay processes. In essence, it represents production of a spin one particle and its following decay. It is violated by electroweak corrections which contain interaction of the initial quarks and final state leptons. It is also modified for the $\gamma\gamma \to \ell^+\ell^-$ scattering process. These corrections are however small at the Z-pole region and neglected in the following. For the measurements insensitive to the azimuthal angle ϕ and forward-backward asymmetry in $\cos\theta$, the most important coefficient is A_0. The coefficient vanishes for $p_T \to 0$ and saturates at $A_0 = 1$ for $p_T \gg 100$ GeV.

The coefficients $A_i(p_T, y_{\ell\ell}, m_{\ell\ell})$ can be calculated using fixed-order predictions. It is possible that the A_2 coefficient is sensitive to non-perturbative effects at low p_T [20], however this should have a small impact on the acceptance. It was demonstrated in Ref. [21] which compared predictions for the A_i coefficients to the data obtained by the ATLAS and CMS collaborations [22, 23]. The calculations were performed at LO ($O(\alpha_S)$), NLO ($O(\alpha_S^2)$) and NNLO ($O(\alpha_S^3)$) order for the Z-boson plus jet process, as provided by the NNLOJET program [24]. For the coefficient A_0, good perturbative convergence is observed with already LO predictions being in reasonable agreement with the data.

Given the $p_T, y_{\ell\ell}, m_{\ell\ell}$ values and the A_i coefficients, the kinematics of the final state leptons and thereby the fraction of events passing fiducial cuts is fully determined. Any fixed-order prediction for the Z boson plus jet process must obey decomposition of equation 1. Therefore, the fiducial acceptance for each $p_T, y_{\ell\ell}, m_{\ell\ell}$ bin can be determined at fixed order, provided it is narrow enough to neglect the p_T dependence inside the bin. The residual theoretical uncertainties arising in this procedure can be estimated the usual way, by PDF and scale variations.

The corrected to the full phase space cross section can be integrated in p_T to provide the full phase space measurement as a function of $y_{\ell\ell}$ and $m_{\ell\ell}$ to be compared to corresponding predictions. The main advantage of this procedure compared to the standard approach that it eliminates dependence on the p_T distribution in predictions which is poorly modeled at fixed order: the p_T dependence as measured in data is used instead.
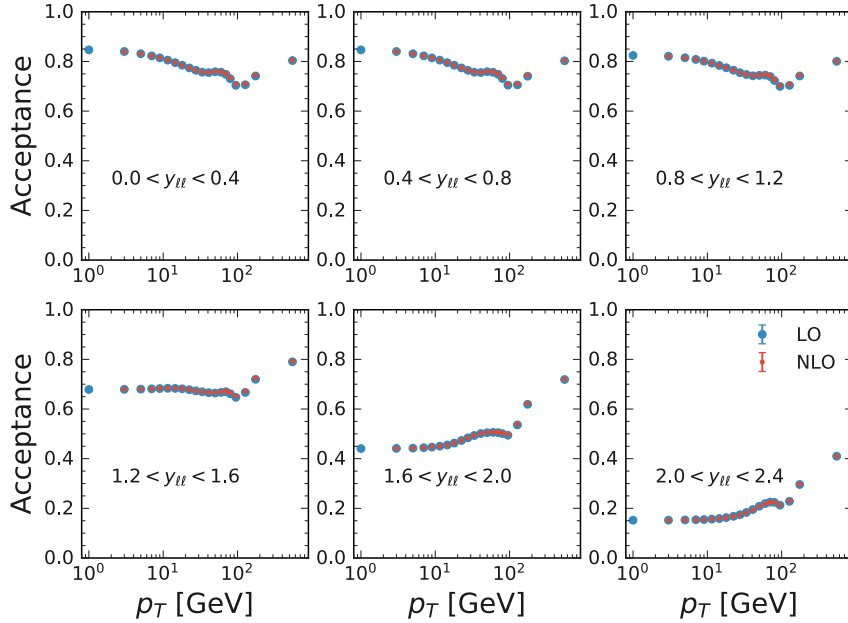
FIG. 1: Fiducial acceptance calculated at LO ($O(\alpha_S)$) and NLO ($O(\alpha_S^2)$) using Z-boson plus jet process. The error bars show total uncertainties of the calculation.

III.   RESULTS

The correction procedure is tested using the ATLAS γ^*/Z data at $\sqrt{s} = 8$ TeV [15]. The cross sections in this analysis are measured differentialy in p_T and $y_{\ell\ell}$ for the $66 < m_{\ell\ell} < 115$ GeV invariant mass range. There are 20 variable-size bins in p_T, starting with narrow 2 GeV bins for low p_T and ending with a wide 700 GeV bin from 200 to 900 GeV. The 6 bins in $y_{\ell\ell}$ are equidistant spanning from 0 to 2.4 with a step of $\Delta y_{\ell\ell} = 0.4$. The measurement is performed in the fiducial space defined by the lepton transverse momentum $p_T^\ell > 20$ GeV and $|\eta_\ell| < 2.4$ requirements. All data tables are taken from the HEPDATA record of the ATLAS publication. Following Refs. [25, 26], the measurement is re-scaled by the original and updated luminosity ratio: 20.3/20.2. The total normalization uncertainty of the measurement is 1.9%.

The fiducial acceptance is estimated using the MCFM v6.8 program interfaced to APPLGRID, for fast evaluation of theoretical uncertainties. The Z plus jet process is computed at LO and NLO yielding acceptance estimates A_{LO} and A_{NLO}, respectively. It is

also possible to use NNLO calculations for the Z plus jet process which became available recently [27], however they are not used in the present analysis. Note that in order of α_S, the NLO calculations for the Z plus jet process match NNLO calculations for inclusive Z-boson production.

The renormalization and factorization scales are set to $m_{\ell\ell}$ and the CT14NNLO PDF set [28] is used for the calculations. The jet transverse momentum is required to be above 1 GeV. The resulting fiducial acceptance is shown in figure 1. The statistical uncertainties for the LO calculations are negligible and for NLO they are below 0.1% for the majority of the bins. To achieve this accuracy, computational resources of about 20000 CPU hours are required.

The fiducial acceptance is very similar for the three central rapidity bins with $y < 1.2$ and it is always above 70%. For the forward rapidity, the acceptance starts to decrease and drops below 20% for the $2.0 < y_{\ell\ell} < 2.4$ bin at low p_T. The p_T dependence of the acceptance is also different for forward compared to central rapidities. The first bin in p_T spans between 0 and 2 GeV and NLO calculations of the acceptance become unstable, thus only the LO result is presented. For all other bins, LO and NLO calculations agree very well.

Figure 2 presents quantitative comparison of the acceptances computed at different orders in terms of $\delta = A_{\mathrm{NLO}}/A_{\mathrm{LO}} - 1$. The NLO correction is below 0.1% for $p_T < m_Z$, where m_Z is the Z-boson mass, for all rapidity bins with $y_{\ell\ell} < 2.0$. For all bins the correction does not exceed 1%, indicating good convergence of the perturbative series. Based on this good agreement and moderate dependence of the correction on p_T, the correction for the bin $0 < p_T < 2$ GeV is estimated using LO calculation, re-scaled by the ratio of NLO to LO for the bin $2 < p_T < 4$ GeV.

Figure 3 shows PDF and scale uncertainties of the acceptance. The PDF uncertainties are evaluated using the CT18ANNLO set [29, 30] scaled to 68% c.l. The scale uncertainties are estimated by varying factorization and renormalization scale by factor of two and taking the envelope of resulting acceptance factors. Both PDF and scale uncertainties are typically below 0.1%. The PDF uncertainties increase to about 0.15% for the highest rapidity bin. As an additional check of the PDF dependence, the acceptance is calculated using CT14NNLO, MMHT14NNLO [31], NNPDF31 [32], ABMP16 [33] and ATLASepWZ16 [3] PDF sets. For all sets except ATLASepWZ16, the calculated acceptance is found to be within the the PDF error bands of the CT18ANNLO set. The ATLASepWZ16 based acceptance agrees with the
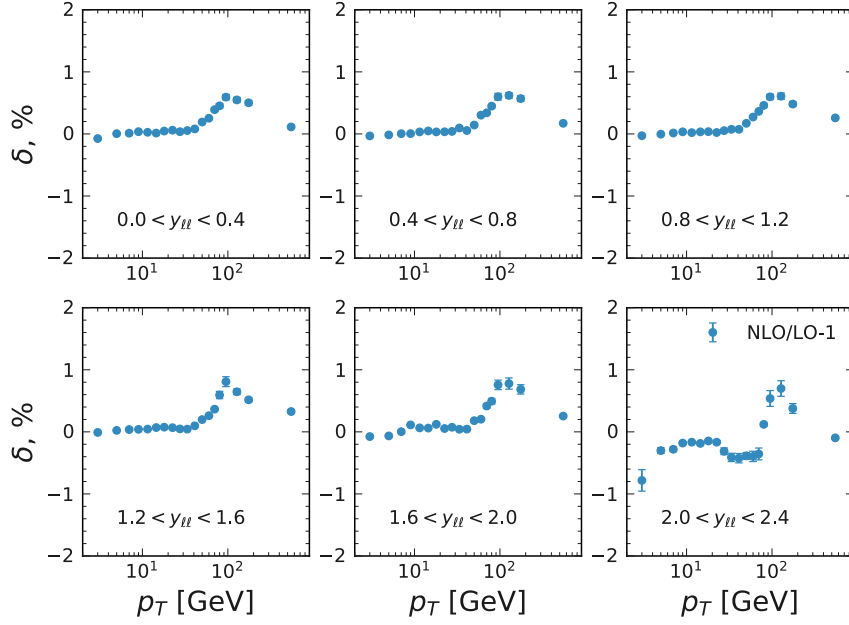
FIG. 2: Percentage difference between acceptance corrections calculated at NLO and LO. The error bars indicate total uncertainties of the NLO calculations.
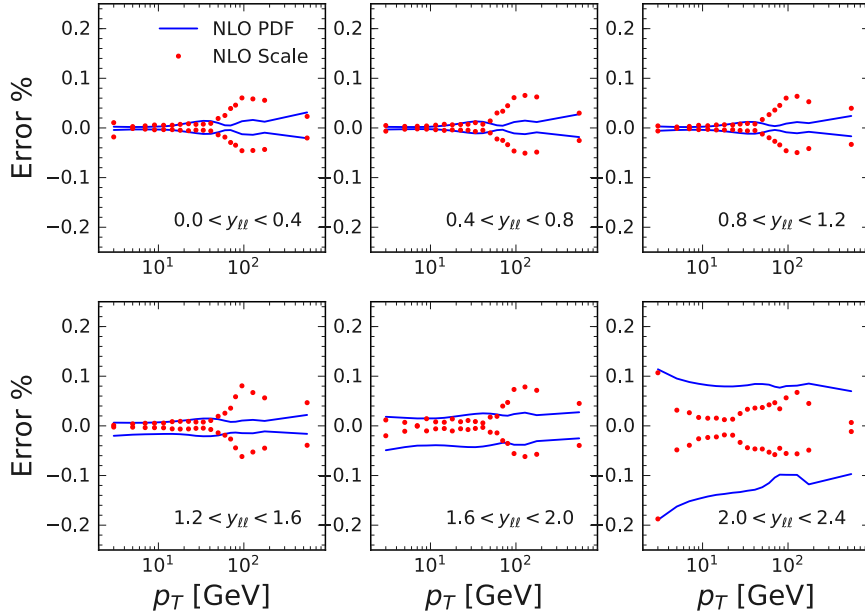

FIG. 3: PDF and scale variation uncertainties of the acceptance correction calculated at NLO.
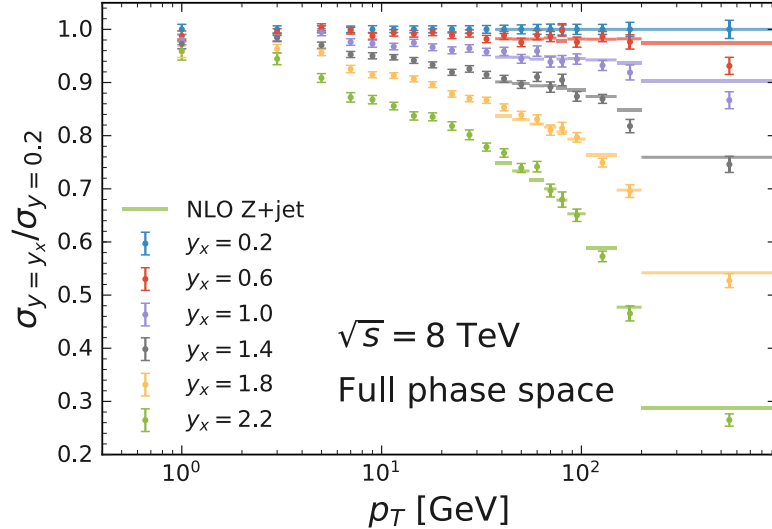
FIG. 4: Ratios of differential $\mathrm{d}\sigma/\mathrm{d}p_T^{\ell\ell}$ full phase space distributions for different $y_{\ell\ell}$ bins to the $0 < y_{\ell\ell} < 0.4$ bin. The error bars show total uncertainties of individual $\mathrm{d}\sigma/\mathrm{d}p_T^{\ell\ell}$ measurements. The horizontal lines shown for $p_T > 35$ GeV represent NLO predictions for Z plus jet process using CT14NNLO PDF set.

other sets for $y_{\ell\ell} < 2$. For the highest rapidity bin, the acceptance based on ATLASepwz16 deviates by as much as -0.2% for low p_T and up to $+0.35\%$ for p_T around m_Z. No additional uncertainty is introduced due to this deviation.

The size of the theoretical uncertainties on the acceptance corrections suggests that it is possible to proceed with applying them to the data. Figure 4 shows the ratio of the $\mathrm{d}\sigma/\mathrm{d}p_T$ distributions corrected to the full phase space for a given $y_{\ell\ell}$ bin to the most central $0 < y_{\ell\ell} < 0.4$ bin. The ratio is close to one for small p_T decreasing almost linearly for large p_T and large $y_{\ell\ell}$. For $p_T > 35$ GeV, the data are compared to fixed-order predictions at NLO for the Z-boson plus jet process computed using the same APPLGRID as for the acceptance correction which is convoluted with the CT14NNLO PDF set. The data and predictions are found to be in reasonable agreement.

As the next step the data are integrated in p_T. The correlated uncertainties are propagated linearly while statistical uncertainties are combined in quadrature. The uncertainty decomposition is shown in figure 5. The uncertainties are dominated by the correlated experimental errors. The statistical uncertainties are at around 0.1% except the highest rapidity
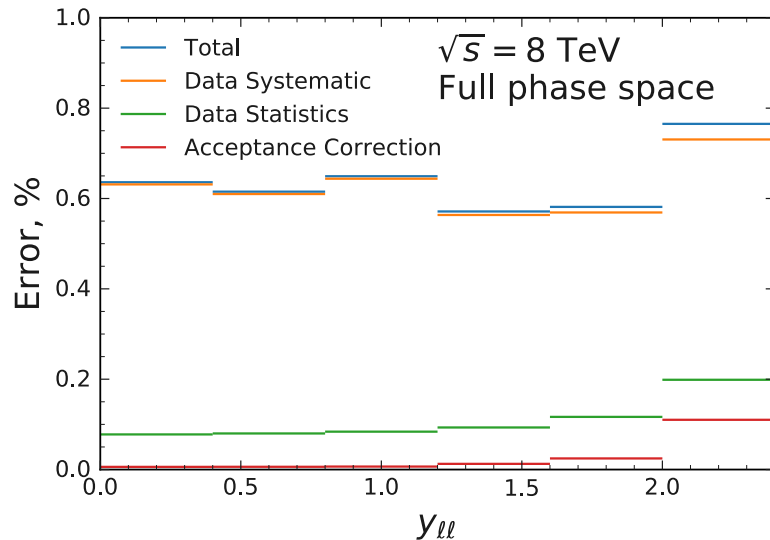
FIG. 5: Decomposition of the uncertainties for the $d\sigma/dy_{\ell\ell}$ measurement. The global normalization uncertainty due to the luminosity measurement of 1.9% is not shown.

bin. The acceptance correction uncertainties are sub-dominant, they are below 0.02% for all but the last bin where they are about 0.1%, dominated by the PDF uncertainty.

The measurements are compared to NNLO predictions obtained using the MCFM v9 program. Two PDF sets are used for the comparison: CT14NNLO and ATLASepWZ16. CT14NNLO is representative of other global PDF sets with reduced compared to $\bar{u}$ and $\bar{d}$ strange-quark distribution. ATLASepWZ16, on the other hand, is obtained by fitting the ATLAS fiducial W, Z data at $\sqrt{s} = 7$ TeV from Ref. [3] and has enhanced strangeness. The MCFM program is used with nominal settings, electroweak corrections disabled, and scales set to $m_{\ell\ell}$. The central value of the total cross section for $\sqrt{s} = 8$ TeV and $66 < m_{\ell\ell} < 116$ GeV obtained for the CT14NNLO PDF set is 1114.9(1) pb, which is 0.4% larger than the value of 1110(1) pb obtained in Ref. [26] using the DYTURBO program [34].

The comparison between the full phase space measurement of $d\sigma/dy_{\ell\ell}$ at $\sqrt{s} = 8$ TeV and predictions is shown in figure 6. The global normalization uncertainty of 1.9% is omitted from the figure and the predictions are shown with PDF uncertainties only. The uncertainties are larger for the CT14NNLO compared to ATLASepWZ16-EIG PDF set due to usage of increased tolerance factors compared to the $\Delta\chi^2 = 1$ criterion adapted for the ATLASepWZ16-EIG set. The predictions based on CT14NNLO (ATLASepWZ16) underes-
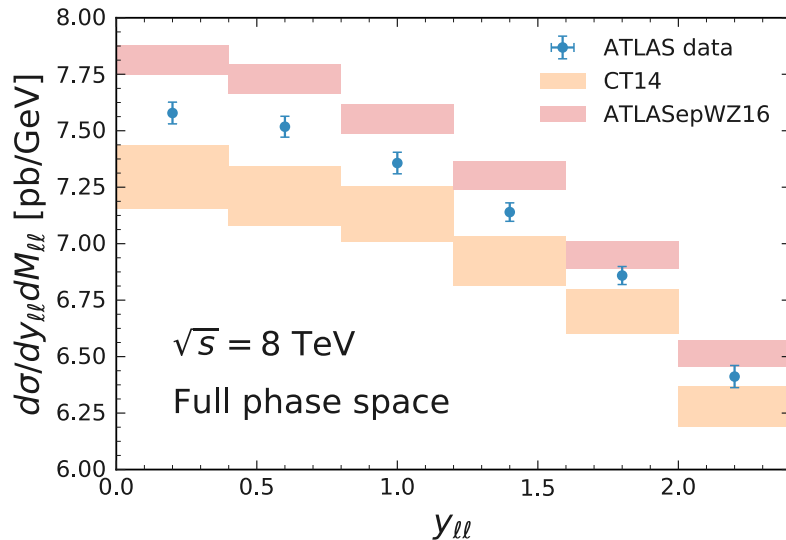
9

FIG. 6: Full phase space measurement of $\mathrm{d}\sigma/\mathrm{d}y_{\ell\ell}$ compared to predictions using various PDFs computed at NNLO using MCFM v9. Global normalization uncertainty of 1.9% is not shown. Error bars show total data uncertainties. Bands indicate PDF uncertainties of the predictions. For ATLASepWZ16, the uncertainties are computed using the ATLASepWZ16-EIG set only.

timate (overestimate) the data. Given the significant global normalization uncertainty the difference is however not significant.

More quantitatively, the comparison can be performed by taking ratios of the predictions to the data. It is also interesting to compare the ratios of the full cross sections to the ratios of the fiducial cross sections, to see the impact of the p_T-dependent acceptance corrections. The fiducial cross section in data is computed by simple integration over the differential cross section. It is verified that the total fiducial cross section agrees with the one reported in the ATLAS publication. The NNLO predictions are obtained using the MCFM v9 program with fiducial cuts enabled. The resulting full and fiducial cross-section ratios for the two PDF sets are shown in figure 7. For the CT14NNLO based prediction, the ratio of the full phase space cross sections is closer to the unity compared to the ratio of the fiducial cross sections. The dependence of the ratio on $y_{\ell\ell}$ is also reduced significantly. For the ATLASepWZ16 based prediction, the fiducial ratio is closer to unity, which is not too surprising since the set is fitted to the fiducial ATLAS measurement at $\sqrt{s} = 7$ TeV. The difference between full and fiducial ratios is similar for both predictions for the five $y_{\ell\ell} < 2.0$ bins. For the first
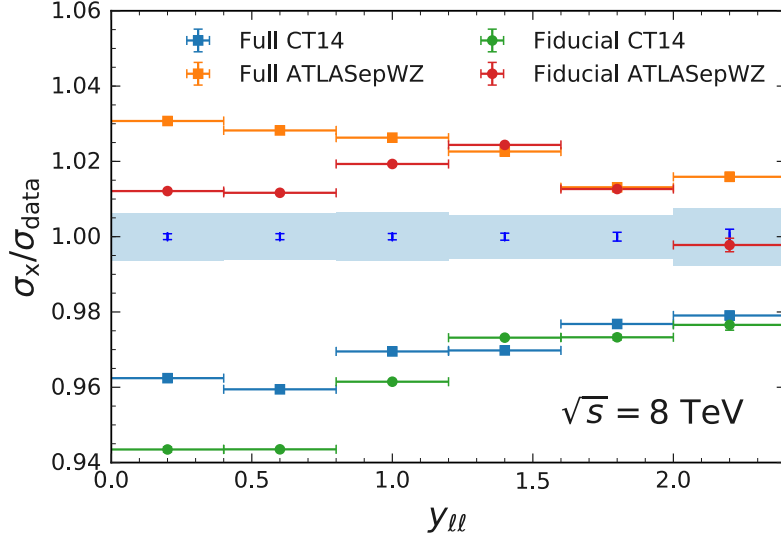
FIG. 7: Ratio of the predicted to the measured $d\sigma/dy_{\ell\ell}$ cross section. The ratios are calculated in the full or fiducial phase space using the CT14NNLO and ATLAS-epWZ PDF sets, as indicated in the legend. The error band (bars) centered at one shows the data total experimental (statistical) uncertainty. The error bars for the ratios of the data to predicted cross sections show estimated statistical uncertainties of the predictions. Global normalization uncertainty of 1.9% is not shown.

three bins the fiducial ratio is lower than the full one, by as much as 2%, for the two lowest y bins. For bins with $1.2 < y_{\ell\ell} < 2.0$, they roughly agree. For the highest rapidity bin, the behavior is different depending on the PDF set. For the CT14NNLO based prediction the two ratios agree while for the ATLASepWZ16 based prediction the fiducial ratio is below the full one by almost 2%.

For the full phase space comparison based on the CT14NNLO and ATLASepWZ16 sets, the ratios of $\sigma_{\text{theory}}/\sigma_{\text{data}}$ show opposite trend as a function of $y_{\ell\ell}$. Given that the strange-quark distribution affects low rapidity region more, based on this observation, it is possible to make a conjecture that the ATLAS data may prefer somewhat larger strangeness content than in the CT14NNLO set and somewhat smaller than in the ATLASepWZ16 set. The overshoot of the predictions based on the ATLASepWZ16 set is likely to be caused by the bias in the fiducial NNLO prediction which was used in the analysis of the ATLAS data at $\sqrt{s} = 7$ TeV.

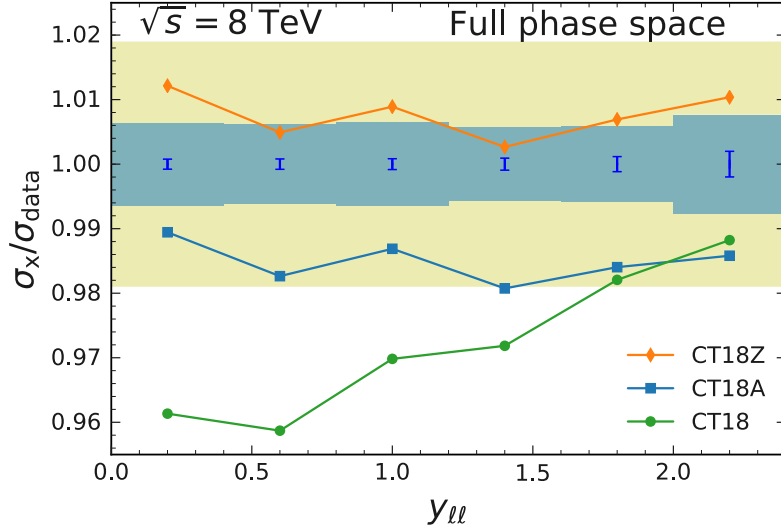To check this, predictions based on CT18NNLO, CT18ANNLO and CT18ZNNLO PDF

FIG. 8: Ratio of the predicted to the measured $d\sigma/dy_{\ell\ell}$ cross section. The ratios are calculated in the full phase space using the CT18, CT18A and CT18Z NNLO PDF sets, as indicated in the legend. The error bands and error bars centered at one show the data normalisation, total experimental (excluding normalisation) and statistical uncertainty.

sets [29, 30] are compared to the data in the full phase space. The results are shown in figure 8. Compared to the CT18NNLO set, both CT18ANNLO and CT18ZNNLO sets include the ATLAS W, Z data at $\sqrt{s} = 7$ TeV. As a result, the CT18ANNLO and CT18ZNNLO sets have an enhanced strange-quark distribution, with no suppression compared to other light quarks for Bjorken $x < 0.01$. The enhancement is however smaller compared to the ATLASepWZ16 set since the CT18 sets use other data which favour smaller strangeness. The strange-quark distribution in CT18NNLO is similar to CT14NNLO. The CT18ANNLO set in addition uses a charm-quark mass that is increased compared to other PDF sets. This leads to suppression of the charm-quark contribution, compensated by an increase of the light-quark sea, yielding in turn an increase of the Drell-Yan cross sections at the LHC, as it was demonstrated in Ref. [35]. The predictions based on the CT18ANNLO and CT18ZNNLO sets show better agreement with the ATLAS data compared to those based on the CT18NNLO set: the ratio shows no dependence on $y_{\ell\ell}$ and the overall normalisation of the ratio is closer to unity.

IV.   DISCUSSION

In the discussion above, it is argued that for comparison of fixed-order predictions with data, it is better to use full

$$\sigma_{\text{full,theory}} = \int \frac{\mathrm{d}\sigma_{\text{theory}}}{\mathrm{d}p_T}\mathrm{d}p_T \quad \text{vs} \quad \sigma_{\text{full,data}} = \int \frac{\mathrm{d}\sigma_{\text{data}}}{\mathrm{d}p_T}\frac{1}{A(p_T)}\mathrm{d}p_T \,, \tag{2}$$

instead of fiducial cross sections

$$\sigma_{\text{fidu,theory}} = \int \frac{\mathrm{d}\sigma_{\text{theory}}}{\mathrm{d}p_T}A(p_T)\mathrm{d}p_T \quad \text{vs} \quad \sigma_{\text{fidu,data}} = \int \frac{\mathrm{d}\sigma_{\text{data}}}{\mathrm{d}p_T}\mathrm{d}p_T \,. \tag{3}$$

Both formula require accurate prediction for the acceptance $A(p_T)$, however equation 2 does not require accurate modeling of the p_T distribution by the prediction. Moreover, the acceptance $A(p_T)$ is well-known for fixed-order predictions with the residual theoretical uncertainties being significantly smaller than the current experimental errors. For future, more accurate experimental measurements, the scale uncertainty may be reduced by using existing higher order calculations. If needed, the PDF uncertainty can be reduced further too, by using the same PDF in the calculation of $\sigma_{\text{full,theory}}$ and $A(p_T)$. This could be relevant for PDF fits in particular and can be arranged without difficulty since the PDF-dependent acceptance $A(p_T)$ can be computed using exact and fast methods such as APPLGRID.

The method is applicable to the measurements differential in the boson transverse momentum p_T. It is natural for Z-boson production, but can be extended for the W boson too. Given that $A(p_T)$ has only mild variation at low p_T (see figure 1), it is probably possible to use coarser p_T binning, which is required by the experimental resolution. Since the rapidity of the W boson can not be reconstructed, this may lead to increased PDF dependence of the acceptance correction factor, requiring its update when performing comparisons for predictions based on different PDFs. Studies of the defiducialization method for W-boson production are however beyond the scope of the current analysis and they await for experimental measurements, such as of the lepton pseudorapidity distribution, reported in bins of the W-boson transverse momentum.

V.   SUMMARY

In summary, a method is proposed to perform comparisons of experimental data on Drell-Yan production, performed in fiducial phase space, and fixed-order QCD predictions with

13

improved accuracy. The method requires the data to be measured differentially in the boson transverse momentum p_T in addition to other variables of interest such as $y_{\ell\ell}$ and $m_{\ell\ell}$. It relies on the ability to calculate the fiducial acceptance correction for a given p_T value at fixed order.

The method is applied to the ATLAS Z-boson production data at a center-of-mass energy of 8 TeV. The uncertainty on the acceptance correction is shown to be small compared to the current level of experimental uncertainties. The data are integrated in p_T and compared to the NNLO predictions. To check impact of the new approach, the comparison is also performed using fiducial cross sections. A significant, compared to experimental uncertainties, improvement in the data description by the predictions based on CT14NNLO set is observed when performing comparison in the full phase space.

VI.   ACKNOWLEDGEMENTS

References

[1] ATLAS Collaboration, M. Aaboud et al., *Measurement of the W-boson mass in pp collisions at $\sqrt{s} = 7$ TeV with the ATLAS detector*, Eur. Phys. J. **C78** (2018) no. 2, 110, arXiv:1701.07240 [hep-ex]. [Erratum: Eur. Phys. J.C78,no.11,898(2018)].

[2] CMS Collaboration, A. M. Sirunyan et al., *Measurement of the weak mixing angle using the forward-backward asymmetry of Drell-Yan events in pp collisions at 8 TeV*, Eur. Phys. J. **C78** (2018) no. 9, 701, arXiv:1806.00863 [hep-ex].

[3] ATLAS Collaboration, M. Aaboud et al., *Precision measurement and interpretation of inclusive W^+ , W^- and Z/γ^* production cross sections with the ATLAS detector*, Eur. Phys. J. **C77** (2017) no. 6, 367, arXiv:1612.03016 [hep-ex].

[4] C. Anastasiou, L. J. Dixon, K. Melnikov, and F. Petriello, *Dilepton rapidity distribution in the Drell-Yan process at NNLO in QCD*, Phys. Rev. Lett. **91** (2003) 182002, `arXiv:hep-ph/0306192 [hep-ph]`.

[5] C. Anastasiou, L. J. Dixon, K. Melnikov, and F. Petriello, *High precision QCD at hadron colliders: Electroweak gauge boson rapidity distributions at NNLO*, Phys. Rev. **D69** (2004) 094008, `arXiv:hep-ph/0312266 [hep-ph]`.

[6] K. Melnikov and F. Petriello, *The W boson production cross section at the LHC through $O(\alpha_s^2)$*, Phys. Rev. Lett. **96** (2006) 231803, `arXiv:hep-ph/0603182 [hep-ph]`.

[7] S. Catani, L. Cieri, G. Ferrera, D. de Florian, and M. Grazzini, *Vector boson production at hadron colliders: a fully exclusive QCD calculation at NNLO*, Phys. Rev. Lett. **103** (2009) 082001, `arXiv:0903.2120 [hep-ph]`.

[8] S. Catani, G. Ferrera, and M. Grazzini, *W Boson Production at Hadron Colliders: The Lepton Charge Asymmetry in NNLO QCD*, JHEP **05** (2010) 006, `arXiv:1002.3115 [hep-ph]`.

[9] S. Frixione and G. Ridolfi, *Jet photoproduction at HERA*, Nucl. Phys. **B507** (1997) 315–333, `arXiv:hep-ph/9707345 [hep-ph]`.

[10] G. Salam, *Thoughts on QCD for Run 2*, `https://gsalam.web.cern.ch/gsalam/talks/repo/2015-02-ATLAS-Annecy-ATLAS-Salam.pdf`.

[11] S. Catani, D. de Florian, G. Ferrera, and M. Grazzini, *Vector boson production at hadron colliders: transverse-momentum resummation and leptonic decay*, JHEP **12** (2015) 047, `arXiv:1507.06937 [hep-ph]`.

[12] ATLAS Collaboration, M. Aaboud et al., *Measurement of the Drell-Yan triple-differential cross section in pp collisions at $\sqrt{s} = 8$ TeV*, JHEP **12** (2017) 059, `arXiv:1710.05167 [hep-ex]`.

[13] D. M. Walker, *Higher Order QCD Corrections to Electroweak Boson Production at Colliders*. PhD thesis, Durham U., 2019. `http://etheses.dur.ac.uk/13284/`.

[14] CDF Collaboration, T. Aaltonen et al., *First Measurement of the Angular Coefficients of Drell-Yan e^+e^- pairs in the Z Mass Region from $p\bar{p}$ Collisions at $\sqrt{s} = 1.96$ TeV*, Phys. Rev. Lett. **106** (2011) 241801, `arXiv:1103.5699 [hep-ex]`.

[15] ATLAS Collaboration, G. Aad et al., *Measurement of the transverse momentum and ϕ_η^* distributions of DrellYan lepton pairs in protonproton collisions at $\sqrt{s} = 8$ TeV with the*

ATLAS detector, Eur. Phys. J. **C76** (2016) no. 5, 291, `arXiv:1512.02192 [hep-ex]`.

[16] J. M. Campbell and R. K. Ellis, *An Update on vector boson pair production at hadron colliders*, Phys. Rev. **D60** (1999) 113006, `arXiv:hep-ph/9905386 [hep-ph]`.

[17] T. Carli, D. Clements, A. Cooper-Sarkar, C. Gwenlan, G. P. Salam, F. Siegert, P. Starovoitov, and M. Sutton, *A posteriori inclusion of parton density functions in NLO QCD final-state calculations at hadron colliders: The APPLGRID Project*, Eur. Phys. J. **C66** (2010) 503–524, `arXiv:0911.2985 [hep-ph]`.

[18] R. Boughezal, J. M. Campbell, R. K. Ellis, C. Focke, W. Giele, X. Liu, F. Petriello, and C. Williams, *Color singlet production at NNLO in MCFM*, Eur. Phys. J. **C77** (2017) no. 1, 7, `arXiv:1605.08011 [hep-ph]`.

[19] J. Campbell and T. Neumann, *Precision Phenomenology with MCFM*, JHEP **12** (2019) 034, `arXiv:1909.09117 [hep-ph]`.

[20] P. Chiappetta and M. Le Bellac, *Angular Distribution of Lepton Pairs in Drell-Yan Like Processes*, Z. Phys. **C32** (1986) 521.

[21] R. Gauld, A. Gehrmann-De Ridder, T. Gehrmann, E. W. N. Glover, and A. Huss, *Precise predictions for the angular coefficients in Z-boson production at the LHC*, JHEP **11** (2017) 003, `arXiv:1708.00008 [hep-ph]`.

[22] CMS Collaboration, V. Khachatryan et al., *Angular coefficients of Z bosons produced in pp collisions at $\sqrt{s}$ = 8 TeV and decaying to $\mu^+\mu^-$ as a function of transverse momentum and rapidity*, Phys. Lett. **B750** (2015) 154–175, `arXiv:1504.03512 [hep-ex]`.

[23] ATLAS Collaboration, G. Aad et al., *Measurement of the angular coefficients in Z-boson events using electron and muon pairs from data taken at $\sqrt{s}$ = 8 TeV with the ATLAS detector*, JHEP **08** (2016) 159, `arXiv:1606.00689 [hep-ex]`.

[24] A. Gehrmann-De Ridder, T. Gehrmann, E. W. N. Glover, A. Huss, and T. A. Morgan, *Precise QCD predictions for the production of a Z boson in association with a hadronic jet*, Phys. Rev. Lett. **117** (2016) no. 2, 022001, `arXiv:1507.02850 [hep-ph]`.

[25] ATLAS Collaboration, M. Aaboud et al., *Luminosity determination in pp collisions at $\sqrt{s}$ = 8 TeV using the ATLAS detector at the LHC*, Eur. Phys. J. **C76** (2016) no. 12, 653, `arXiv:1608.03953 [hep-ex]`.

[26] ATLAS Collaboration, M. Aaboud et al., *Measurements of top-quark pair to Z-boson cross-section ratios at $\sqrt{s}$ = 13, 8, 7 TeV with the ATLAS detector*, JHEP **02** (2017) 117,

arXiv:1612.03636 [hep-ex].

[27] A. Gehrmann-De Ridder, T. Gehrmann, N. Glover, A. Huss, and T. A. Morgan, *NNLO QCD corrections for Z boson plus jet production*, PoS **RADCOR2015** (2016) 075, arXiv:1601.04569 [hep-ph].

[28] S. Dulat, T.-J. Hou, J. Gao, M. Guzzi, J. Huston, P. Nadolsky, J. Pumplin, C. Schmidt, D. Stump, and C. P. Yuan, *New parton distribution functions from a global analysis of quantum chromodynamics*, Phys. Rev. **D93** (2016) no. 3, 033006, arXiv:1506.07443 [hep-ph].

[29] T.-J. Hou et al., *Progress in the CTEQ-TEA NNLO global QCD analysis*, arXiv:1908.11394 [hep-ph].

[30] T.-J. Hou et al., *New CTEQ global analysis of quantum chromodynamics with high-precision data from the LHC*, arXiv:1912.10053 [hep-ph].

[31] L. A. Harland-Lang, A. D. Martin, P. Motylinski, and R. S. Thorne, *Parton distributions in the LHC era: MMHT 2014 PDFs*, Eur. Phys. J. **C75** (2015) no. 5, 204, arXiv:1412.3989 [hep-ph].

[32] NNPDF Collaboration, R. D. Ball et al., *Parton distributions from high-precision collider data*, Eur. Phys. J. **C77** (2017) no. 10, 663, arXiv:1706.00428 [hep-ph].

[33] Alekhin, S. and Blümlein, J. and Moch, S. and Placakyte, R., *Parton distribution functions, α_s, and heavy-quark masses for LHC Run II*, Phys. Rev. **D96** (2017) no. 1, 014011, arXiv:1701.05838 [hep-ph].

[34] S. Camarda et al., *DYTurbo: Fast predictions for Drell-Yan processes*, arXiv:1910.07049 [hep-ph].

[35] H1, ZEUS Collaboration, H. Abramowicz et al., *Combination and QCD Analysis of Charm Production Cross Section Measurements in Deep-Inelastic ep Scattering at HERA*, Eur. Phys. J. **C73** (2013) no. 2, 2311, arXiv:1211.1182 [hep-ex].